



Rice Acreage Delineation in the Nile Delta Based on Thermal Signature

Ramadan Abdelaziz Tolba¹ · Mohammed Ahmed El-Shirbeny² · Samir Masoud Abou-Shleel¹ · Mohsen Ahmed El-Mohandes¹

Received: 21 July 2019 / Accepted: 12 October 2019 / Published online: 29 October 2019
© King Abdulaziz University and Springer Nature Switzerland AG 2019

Abstract

Rice is one of the world's significant food crops, especially in Egypt. The distribution data of planted and harvested paddy rice fields are essential for food security and the management of water resources. The determined area within agricultural associations is often subjective, expensive, labor intensive, time-consuming, and prone to errors. Therefore, this study aimed to determine the paddy rice areas in the Nile Delta using a new methodology based on satellite data. The rice areas could be classified with good results at the beginning of the 1st flooding period applying the Normalized Difference Vegetation Index (NDVI). The temporal profiles of NDVI and Land Surface Temperature (LST) were investigated. The NDVI profiles of different targets were analyzed to differentiate between rice and other crops, but the results failed to distinguish between rice and other crops in all stages after full vegetation cover. However, the analyzed LST profiles indicated the discrimination capability between rice and other crops in all vegetation development stages. The accuracy was high as 97% and 74% for LST and NDVI, respectively. The LST-based classification indicated that the distributed rice fields throughout the study area were 32.7% of the total cultivated area. The accuracy of LST results had an advantage over NDVI.

Keywords GIS · Nile delta · Remote sensing · Rice · Thermal signature · NDVI · LST

1 Introduction

Rice is the primary food and security crop that is cultivated in many countries. This crop describes approximately 15% of the world's total arable land. More than three billion people in the world are considering rice as their basic food source (Siyal et al. 2015). Egypt is the most inclusive rice producer in the Near East area (Abo-State et al. 2014), where rice cultivation requirements a determined place in Egypt, especially in the northern part of the Nile Delta. The prior fact is described as this area constitutes about 95% of the cultivated rice area, while south Delta (i.e., Fayoum and other governorates) occupy only about 3% of the total rice sector. Furthermore, Egyptian central governorates contribute around 2% of rice production. Summer rice estimates for

97% of the total rice zone in Egypt, while Nile rice does not exceed 1% of this region (Arafat et al. 2010; Saleh 2016).

Cropland acreage is a critical variable that brings a broad group of end-users, including policymakers, scientists concentrating on global climate or environmental change and agricultural market drivers (Pan et al. 2012; Liang and Gong 2015). The cultivated region and crop production calculations are usually determined using obtained field data on the ground via agricultural associations affiliated to the Ministry of Agriculture. However, these reports are often subjective, expensive, laborious, time-consuming, and prone to errors that may lead to less accurate estimations. Also, in most countries, data on crop area and yield arrive late for analysis, make inferences, and take proper measures for avoiding food deficits, (Siyal et al. 2015). Consequently, there is an essential need for an automated, conventional, and reliable rice field monitoring method.

Throughout the past decades, remote sensing technique has been considered as a great tool to provide crop mapping as the most common way to obtain the acquire crop acreage maps, (Sakamoto et al. 2014; Zhang et al. 2016). It becomes an essential global tool for identification, monitoring, and forecasting of crop yields as well as acreage

✉ Samir Masoud Abou-Shleel
s_masoud_2006@azhar.edu.eg

¹ Environment and Bio-Agriculture Department, Faculty of Agriculture, Al-Azhar University, Nasr City, Cairo, Egypt

² National Authority for Remote Sensing and Space Sciences (NARSS), Cairo, Egypt

under cultivation, (Siyal et al. 2015). Many investigations have been used for various optical images to producing rice mapping at regional scales with supervised or unsupervised classification techniques, (Li et al. 2012; Zhang et al. 2015). Recently, substantial development has been made to monitor crop phenology based on satellite data. For example, the NOAA/AVHRR and SPOT-VGT were used to classify the phenological date of winter wheat crop in the North China Plain, Liu et al. (2018). Existing algorithms for classifying rice-cultivated areas are based on the individual physical characteristics of rice crop through the transplanting periods and use vegetation index that is sensitive to the pattern of the vegetation and soil moisture content. The effective and multi-temporal satellite remote sensing could be a satisfactory approach to assist decision-makers with an accurate and up-to-date active form of the quantity and the distribution of rice cultivation over the area (Arafat et al. 2010).

In the previous studies, the rice-cultivated areas were estimated based on NDVI only, while in this study, both NDVI and LST will be used to calculate the rice-cultivated areas. NDVI will be used in the first period of the growing season (transplanting period) because the NDVI value reaches its lowest level during this period as a result of soil flooding and low plant density. The LST will be practiced throughout the maturity stage and before the harvest date because of the reduction of LST rates to its lowest level throughout this period due to the increase rice field shading and soil flooding which allows distinguishing the rice fields from other crops.

The included study proposes to determine paddy rice fields in the Egyptian Nile Delta region using the thermal

signature, as a new tool to distinguish rice fields from other cultivated crops.

2 Materials and Methods

2.1 Study Area

The Egyptian Nile Delta covers only about 2% of its area but comprises nearly 63% of its agricultural land (Mabrouk et al. 2013). Rice cultivation takes place in the Egyptian Nile Delta, especially in the northern part as shown in Fig. 1. This area comprises about 95% of the total rice-cultivated area. It covers the area south–north from 30°4' N–31°36' N and east–west from 32°12' E to 29°25' E, (Arafat et al. 2010; Saleh 2016).

2.2 Data Collection

Landsat images were obtained from the USGS earth explorer website (Landsat-8 OLI TIRS) during the period from May 30th to August 18th. Landsat-8 data used in the present study are depicted in Table 1. The data were chosen to be geometrically and atmospherically corrected. The subtraction method (dark-object) was applied to correct the atmosphere effects on reflected data based on Chavez (1996). The image processing was executed using ENVI 5.1 and ArcGIS 10.2 software.

Six hundred field checkpoints were collected using a handheld GPS device during the rice-growing season (June and July 2016) in three governorates describing the western, central and eastern Nile Delta (Behaira, Gharbia, and

Fig. 1 Rice-cultivated areas in Nile Delta

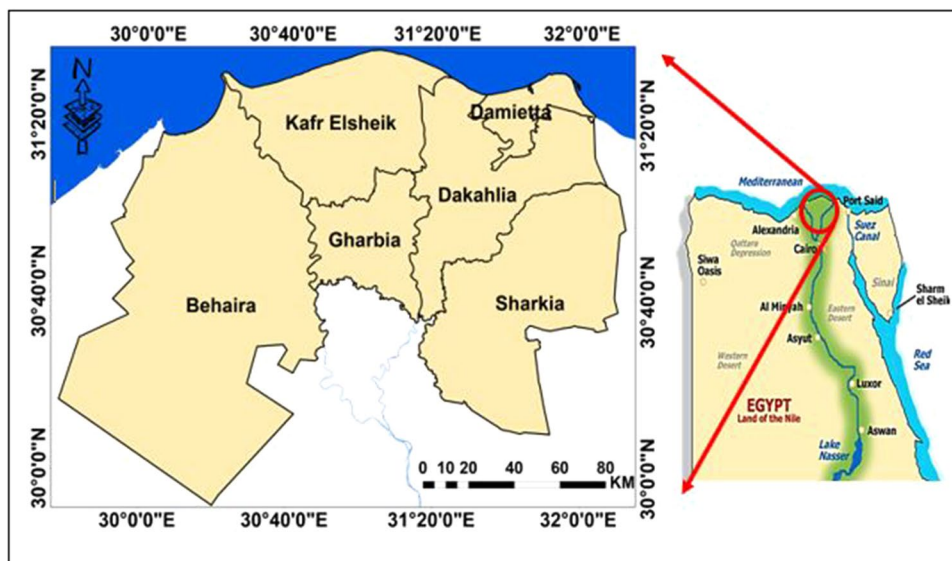
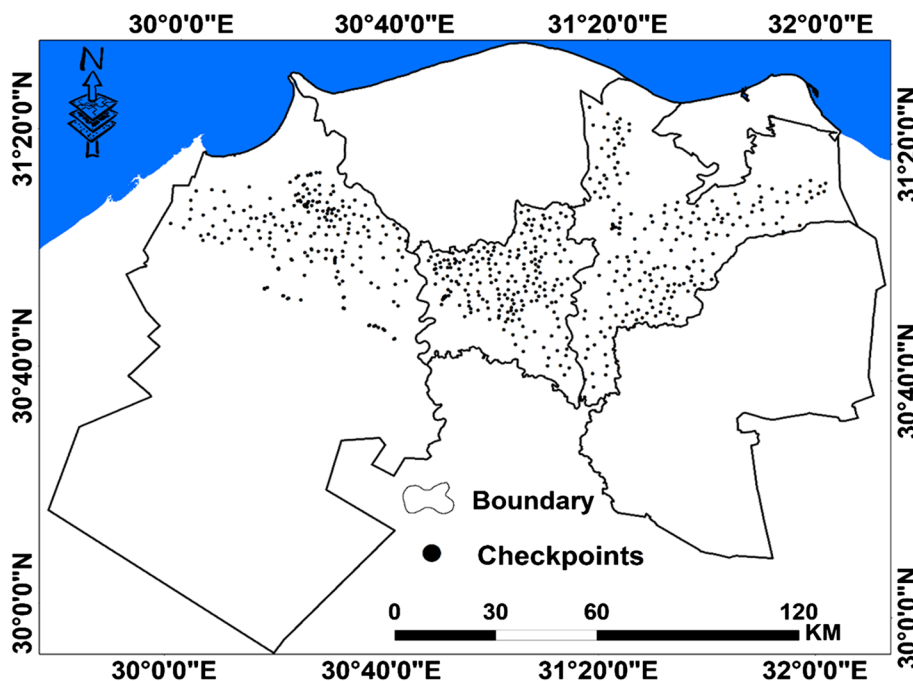


Table 1 Landsat-8 data used in the present study

| Scene no. | Acquisition date | Path | Row | Scene no. | Acquisition date | Path | Row |
|-----------|------------------|------|-----|-----------|------------------|------|-----|
| 1 | 21/4/2016 | 176 | 39 | 11 | 21/4/2016 | 176 | 38 |
| 2 | 14/5/2016 | 177 | 38 | 12 | 14/5/2016 | 177 | 39 |
| 3 | 30/5/2016 | 177 | 38 | 13 | 30/5/2016 | 177 | 39 |
| 4 | 8/6/2016 | 176 | 38 | 14 | 8/6/2016 | 176 | 39 |
| 5 | 15/6/2016 | 177 | 38 | 15 | 15/6/2016 | 177 | 39 |
| 6 | 24/6/2016 | 176 | 38 | 16 | 24/6/2016 | 176 | 39 |
| 7 | 10/7/2016 | 176 | 38 | 17 | 10/7/2016 | 176 | 39 |
| 8 | 17/7/2016 | 177 | 38 | 18 | 17/7/2016 | 177 | 39 |
| 9 | 26/7/2016 | 176 | 38 | 19 | 26/7/2016 | 176 | 39 |
| 10 | 18/8/2016 | 177 | 38 | 20 | 18/8/2016 | 177 | 39 |

Fig. 2 Checkpoints distribution in Behaira, Gharbia and Dakahlia governorates



Dakahlia), to evaluate and examine the satellite data with fieldwork results. The distribution of checkpoints is shown in Fig. 2.

The statistical data of rice crop area in 2016 were collected from Agricultural Statistics, Economic Affairs Sector, Ministry of Agriculture and Land Reclamation, Egypt, to be compared with estimated rice-cultivated areas using satellite data as presented in Fig. 3.

2.3 Image Processing

Landsat data were primarily clipped to exclude untargeted classes from the images for decreasing the processing time and output extent. A mask was then applied to this subset to remove untargeted areas and clouds. Masking of the

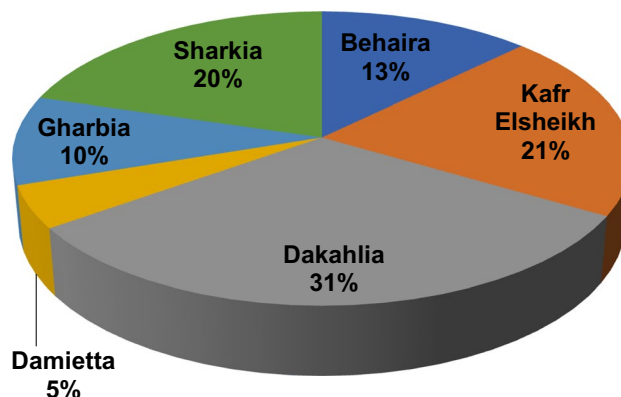


Fig. 3 Rice cultivation area in the Nile Delta during 2016 reported by Economics Affairs Sector

Landsat imagery was performed using ArcGIS software (version10.2).

Satellite data contained numerous optical channels. The visible and near-infrared bands were used to calculate NDVI, while thermal bands were applied to estimate the LST. The radiometric calibration procedure is a common method to adapt optical and thermal satellite data channels from digital number (DN) to radiance and reflectance, correspondingly. The NIR and R were used to detect NDVI as follows:

$$\begin{aligned} \text{NDVI} &= \left[(\text{NIR} - \text{R}) / (\text{NIR} + \text{R}) \right] \\ &= \left[(\text{Band5} - \text{Band4}) / (\text{Band 5} + \text{Band 4}) \right]. \end{aligned}$$

$$\text{NDVI} = \frac{(\text{NIR} - \text{R})}{(\text{NIR} + \text{R})} = \frac{(\text{Band 5} - \text{Band 4})}{(\text{Band 5} + \text{Band 4})}$$

For the thermal channels, the DN values were converted to radiance unit (Rad). The NDVI was used to estimate the emissivity (ϵ_s). based on the developed empirical equation of Valor and Caselles (1996). The Rad was involved to estimate radiant temperature (T_o). The T_o was divided by ϵ_s . to detect the LST.

$$\epsilon_s = 0.9932 + 0.0194 \ln \text{NDVI}$$

The TIRS data can be changed from spectral radiance into the top of atmosphere brightness temperature practicing the thermal constants given in the metadata file according to (USGS):

$$T = K_2 / \left[\ln (K_1 / \text{Red}) + 1 \right],$$

where K_1 and K_2 are satellite coefficients. The K_1 and K_2 coefficients for band 10 were calculated based on 774.89 and 1321.08, respectively.

The LST is estimated as follows:

NDVI and LST were combined to differentiate the rice crop from other crops, where NDVI was used to distinguish both field crops and fruit grown at the same time but have a longer growing season than rice such as cotton, moreover to a small percentage of rice field still immersed in water. LST was used to distinguish rice yield from other field crops that have the same length of planting season and sowing history as maize, since when we observe low LST values during the rice growing season, it enables us to distinguish it from other crops with high accuracy.

2.4 Segmenting Images

Segmentation image is the process of partitioning an image into multiple segments by homogeneity, to modify the reproduction of an image toward something more significant and more satisfactory to investigate. After calculating the land surface temperature, image segmentation was carried out to separate the rice crop from other crops. In thresholding,

pixels are allocated to categories according to the range of values in which a pixel lies (Blaschke et al. 2004). Also, it was used to segment an image into areas of connected pixels based on the pixel DN value.

2.5 Statistical Analysis

The obtained results were subjected to analysis of variance according to the procedure outlined using “SPSS software ver. 20” for Windows 10 following the methods of Steel and Torrie (1980). All evaluations of consequence were carried out based on the Paired *T* Test and correlation factor for the threshold of significance (*p* value) of 5%. Also, descriptive statistics were estimated using Minitab 18.1.

3 Results and Discussion

3.1 Determination of Cultivated Rice Area in the Nile Delta Using Satellite Data

3.1.1 NDVI Values Analysis to Discriminate Rice Fields

Numerous vegetation indices have been used to discriminate crops, i.e., NDVI, EVI (Enhanced Vegetation Index) and SAVI (Soil Adjusted Vegetation Index) through monitoring crop growth stages, crop conditions, and crop density. NDVI is the most widely used. The temporal profiles of vegetation indices records life cycle of rice crop which grows in flooded soils, beside the paddy areas which contains from spots of open water and green rice during the beginning period of the developing stage (transplanting phase), these features can be directly detected based on Chen et al. (2011). The NDVI time-series data have been used to identify numerous crop patterns based on available information and knowledge of the growing period sequence of paddy and other seasonal crops. It could be summarize the methodology and all procedures which followed up during this study as shown in Fig. 4.

The temporal NDVI profiles reflected the rice growth stages (emergence, vegetative growth, and senescence) and growth profiles of other crops (Figs. 5 and 6). Before transplanting, NDVI has low values of 0.23 for bare soil on May 14th. During the transplanting period, rice fields were flooded; hence, the NDVI value decreased to about 0.17 on May 30th. After transplanting, NDVI value was increased rapidly with the growth of rice and reached a peak of 0.89 during the spike differentiation period on Aug. 18th; then NDVI value was decreased after the maturity period with the decrease in water content and photosynthesis activities. After harvest, rice fields turned into the bare soil with an NDVI value of 0.24 on Oct. 14th. These results were in harmony with those obtained by Chen et al. (2011) who found that before transplanting, NDVI has low values of 0.11 for

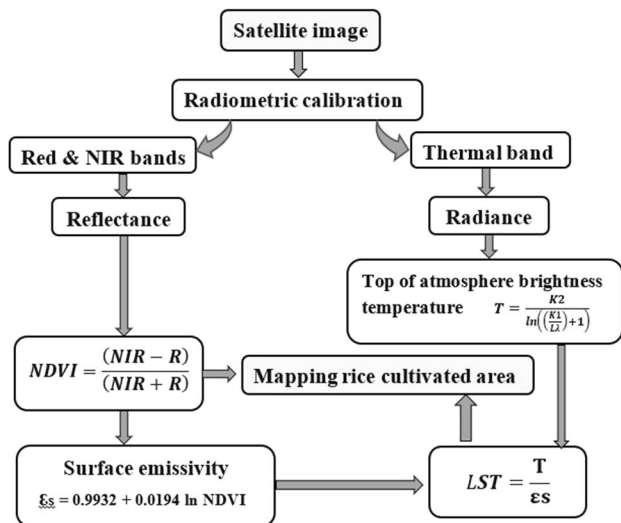


Fig. 4 Flow chart of extracting LST and NDVI from satellite data

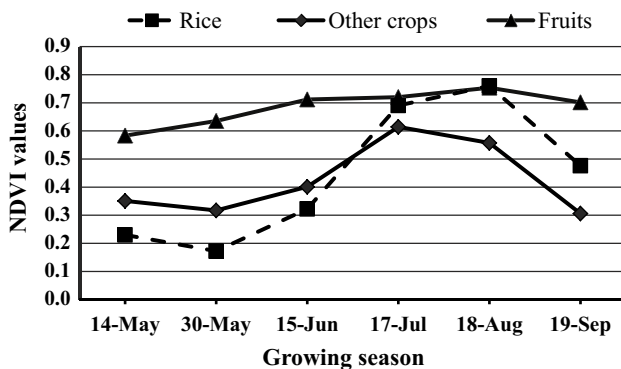


Fig. 5 Temporal variation of NDVI rice fields in the studied area

bare soil. After transplanting, the NDVI value was increased rapidly with the growth of rice and reached a peak during the spike differentiation period. After harvest, rice fields turned into the bare soil with NDVI value of 0.09.

For other ground types, some other crops are planted at a similar period of rice transplanting, but they have a longer life cycle than rice, so that their NDVI values remain high after rice harvests such as cotton and fruit crops. Some other crops that have a life cycle similar to rice, i.e., maize, can be distinguished during the first period of rice cultivation where NDVI values of rice are lower than other crops due to the flooded fields. In this period, the rice fields are immersed with water and are very short, making it challenging to distinguish rice from other crops. The high temporal NDVI profiles suggested that it can be used as a possible factor to discriminate rice fields from other ground types in the study area through their unique phenology and dynamic profiles of NDVI.

3.1.2 LST Analysis to Discriminate Rice Fields

The results presented in Figs. 7 and 8 presented LST rates throughout growing stages (emergence, growth, and senescence) of rice plants. Before transplanting, LST for the rice fields and other crops have high values of 46.0 °C where the soil was bare. During the transplanting period, rice fields were flooded; this relatively decreased LST value to about 40.0 °C on May 30th but still high due to solar heating of rice field water, where the biomass was still weak. Also, for other crops, LST values remained high (42.0 °C) during the same phase. After transplanting, LST value decreased rapidly with rice growth and rice field shading as it reached 31.0 °C after about 2 months of planting on July 17th, while LST values for other crops were 37.0 °C, allowing rice fields to be distinguished from other crops and easily identifiable. As water content and photosynthesis activities decreased in rice fields, the LST value was increased to about 37.0 °C on Sept. 19th. After harvest, the rice fields turned into the bare soil with LST value of 44.0 °C during Oct. For other crops (such as maize and cotton), the lowest temperatures were reached during different growth stages as it was higher than 37.0 °C, which helped to distinguish them from rice. The thermal indices distinguish well between the vegetation, soil, and water, which improve the LULC classification accuracy. The relationship between LST and vegetation indices increased the overall accuracy for land-use/land-cover (LULC) classification by 6%, (Sinha et al. 2015).

The data presented in Table 2 indicated the descriptive statistics including mean, standard deviation, standard error of the mean, minimum, maximum, range, first quartile, median, third quartile and interquartile range (IQR) of NDVI and LST. Also, the box plots of both variables were created as shown in Fig. 9. These data revealed that the NDVI value ranged from 0.0 to 0.72 with a mean of 0.23 ± 0.0042 and median of 0.22. Values above 0.46 were considered outliers according to IQR and presented as whiskers. Also, results of the LST showed that the values ranged from 30.1 to 37.8, with a mean of 32.8 ± 0.054 and median of 32.58. According to IQR, values above 36.3 were considered outliers and presented as whiskers.

The NDVI and LST outliers could be attributed to the different transplanting dates of rice crop in different regions (checkpoint) according to farmers, which leads to an increase in the values of the NDVI in the earlier cultivated areas compared to the other regions. In vice versa, the LST values increased in the later cultivated areas compared to the earlier cultivated areas.

3.1.3 Estimating the Rice-Cultivated Area

A complete statistic of rice-producing governorates in Egypt was produced and mapped to identify the spatial distribution

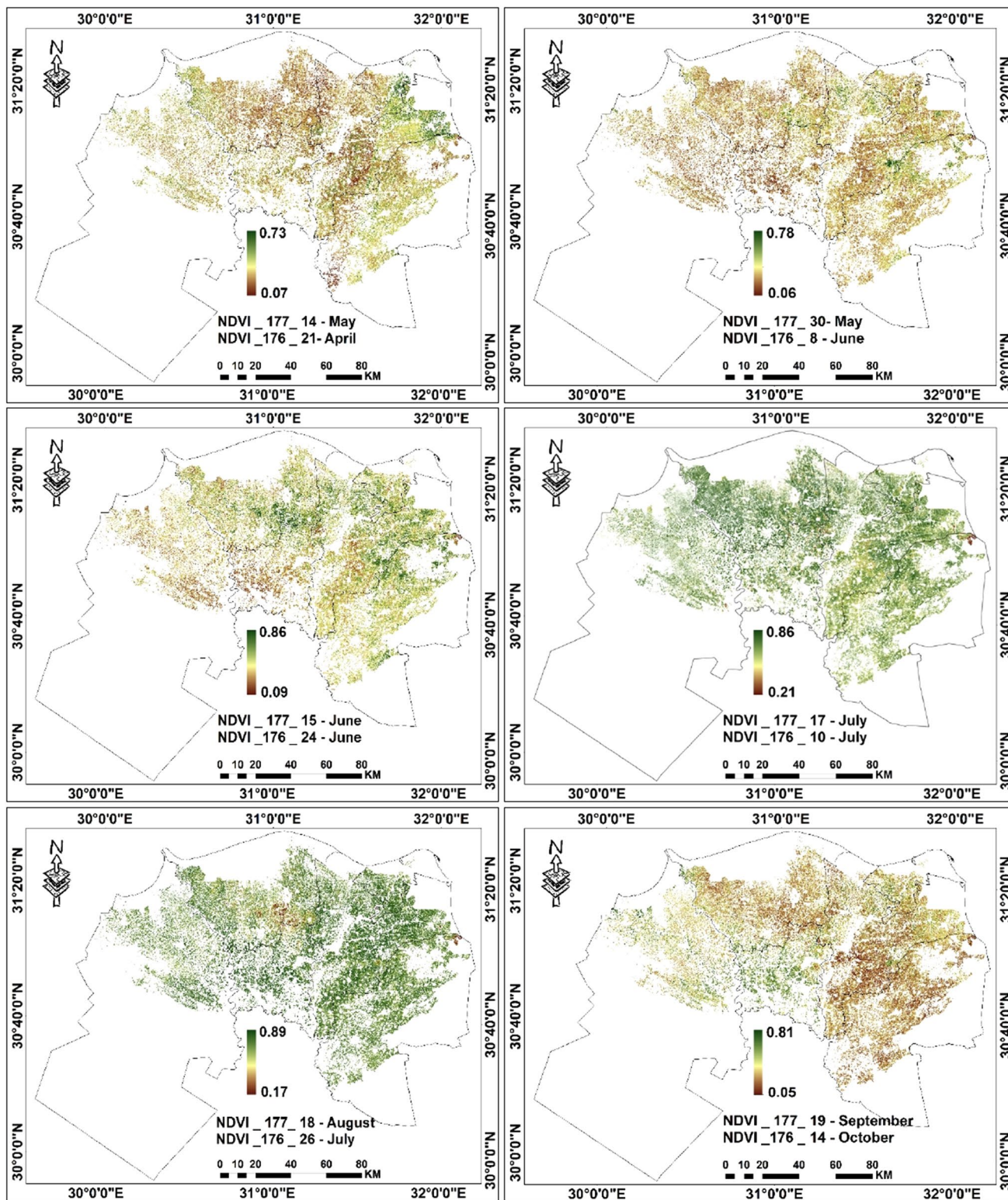


Fig. 6 NDVI for the studied area during rice-growing season

of rice cultivations in each governorate of the Nile Delta, as shown in Fig. 10 and Table 3. The data presented in Fig. 10 showed the spatial distribution of rice cultivation areas in the

Nile Delta governorates during the year 2016 using Landsat-8 data. These obtained data indicated that the rice fields found distributed throughout the studied area with an area

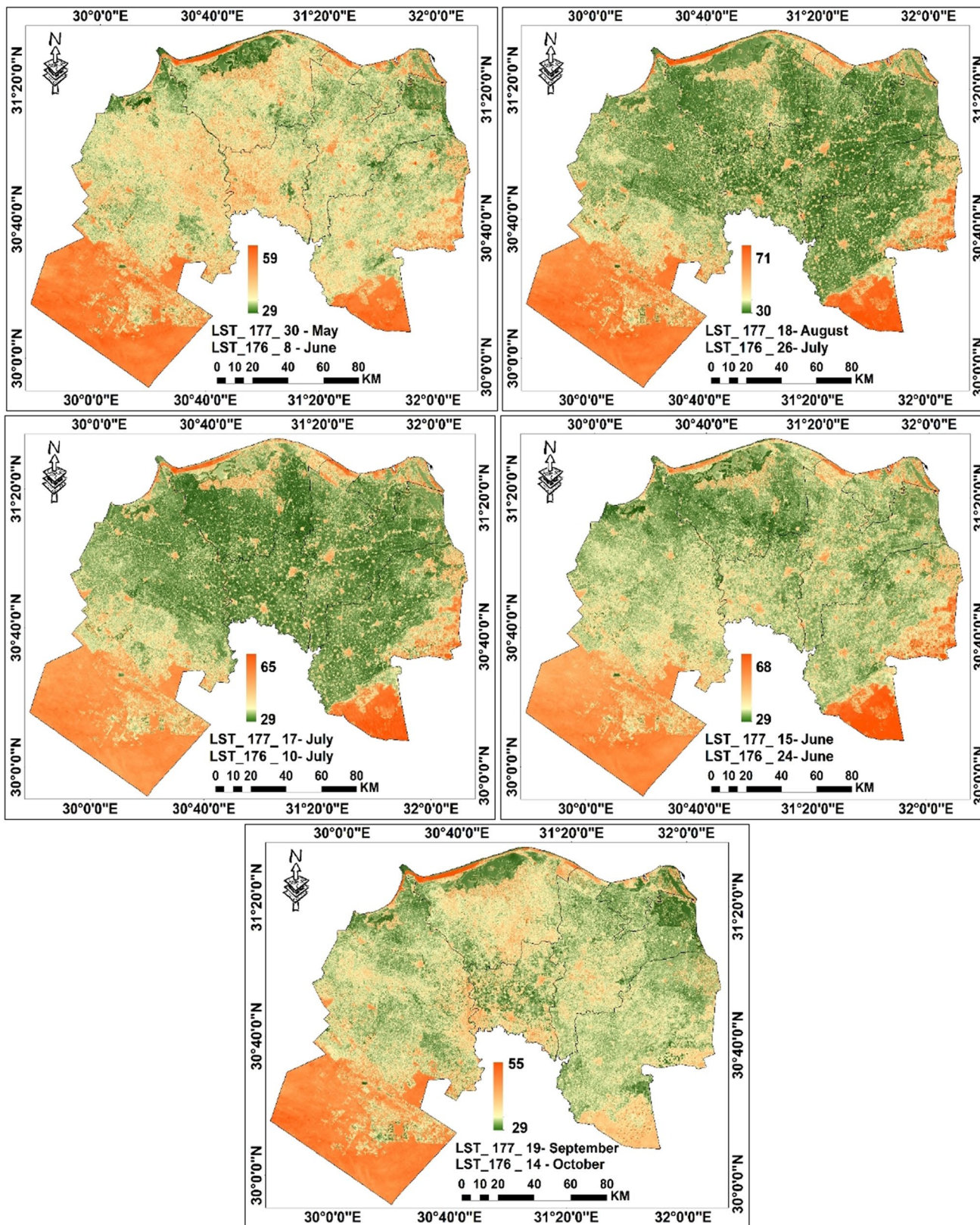


Fig. 8 Temporal variation of LST rice fields in the studied area

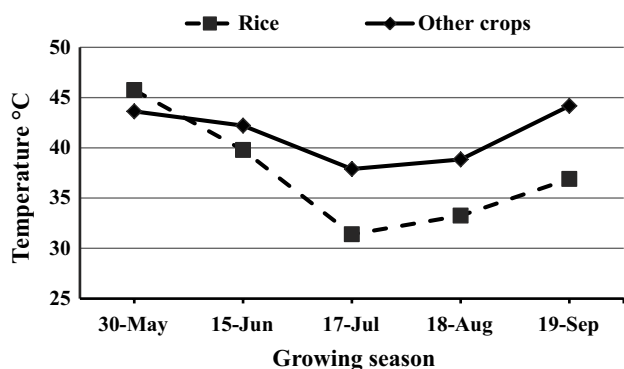


Fig. 7 LST for the studied area during the rice-growing season

of about 1397442.1 feds. Behaira governorate recorded the most extensive boundary and total cultivated area with mean values of 2729498.3 and 1620557.6 fed., respectively (Table 3). Damietta governorate was detected as the lowest boundary area and total cultivated area with mean values of 205339.9 and 106031.2 fed., respectively. Although the governorates of Behaira and Sharkia are considered as the largest in terms of rice cultivation area of the Nile Delta governorates, however, the rice area represented about 7.0 and 23.8% of the total governorate area, respectively, where the most cultivated rice area was concentrated in the northern and north-western parts in these governorates, respectively.

These obtained results could be attributed to the topographic conditions in these parts of the two governorates which are suitable for rice cultivation. Also, the results showed that the total rice-cultivated area in Nile Delta was accounted for 32.7% of total cultivated area in all governorates, as Dakahlia governorate recorded the largest in terms of rice-cultivated area, with mean value of 61.8%, followed by Damietta (55.4%), Kafr Elsheikh (48.6%), Sharkia (34.8%), Gharbia (34.7%) and Behaira (11.9%).

As for the comparison between the governorates in terms of rice-cultivated area, Dakahlia governorate contained the most extensive area (29.5%) of the total rice-cultivated area, followed by Sharkia, Kafr Elsheikh, Behaira, Gharbia and Damietta governorates with mean values of 21.8, 20.6, 13.8, 10.1 and 4.2%, respectively. These results are in agreement with those obtained by Arafat et al. (2010) who found that the Dakahlia governorate contained the largest rice-cultivated area during 2009 with a mean value of 379000.0 feds. In vice versa, Damietta governorate contained the lowest rice-cultivated area with a mean value of 64161.9 feds.

Regarding the comparison between two tools that were used to estimate the rice-cultivated areas in the Nile Delta during 2016, the first tool derived from satellite data and the second one was reported by Economic Affairs Sector—Ministry of Agriculture and Land Reclamation. The data in Table 4 showed that there were no significant differences between these tools, although the cultivated rice areas

Table 2 Descriptive statistics of NDVI and LST at the studied area

| Variable | Mean | SE mean | St dev | Mini. | Q1 | Median | Q3 | Max. | Range | IQR |
|----------|-------|---------|--------|-------|-------|--------|-------|------|-------|------|
| NDVI | 0.23 | 0.004 | 0.10 | 0.00 | 0.16 | 0.22 | 0.28 | 0.72 | 0.72 | 0.12 |
| LST | 32.80 | 0.054 | 1.32 | 30.08 | 31.82 | 32.6 | 33.58 | 37.8 | 7.7 | 1.77 |

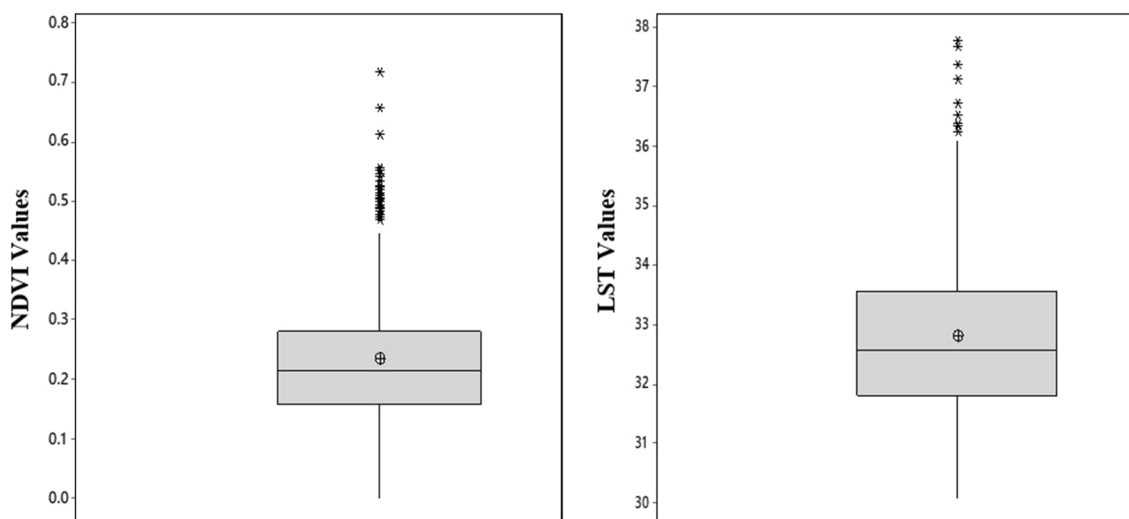
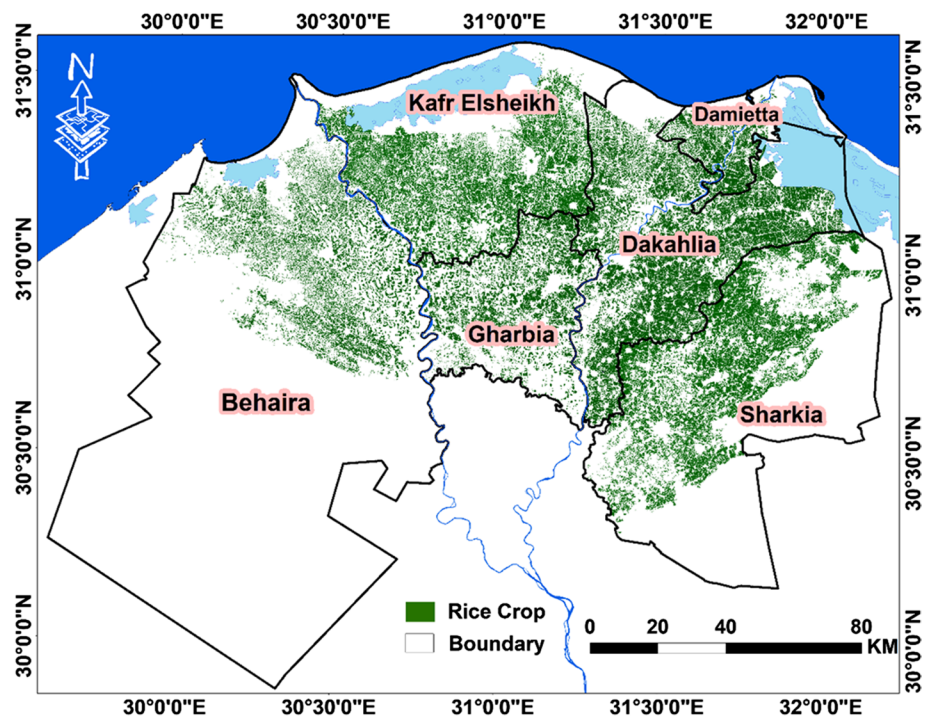


Fig. 9 Box plot of NDVI and LST values (mean is presented as a symbol while the median is presented as a connected line inside the box while outliers are presented as asterisks)

Fig. 10 Rice cultivation over the studied area based on LST**Table 3** Rice cultivation areas in the Nile Delta governorates during 2016

| Governorates | Governorate boundaries (Fed.) | Total cultivated area (Fed.) | Rice-cultivated areas (Fed.) | % Rice area from the total cultivated area | % of each governorate |
|--------------|-------------------------------|------------------------------|------------------------------|--|-----------------------|
| Behaira | 2729498.3 | 1620557.6 | 192810.7 | 11.9 | 13.8 |
| Kafr Elsheik | 909647.1 | 592376.4 | 287708.0 | 48.6 | 20.6 |
| Dakahlia | 929663.9 | 666840.0 | 412041.1 | 61.8 | 29.5 |
| Damietta | 205339.9 | 106031.2 | 58784.5 | 55.4 | 4.2 |
| Gharbia | 475277.6 | 405453.6 | 140790.9 | 34.7 | 10.1 |
| Sharkia | 1280700.6 | 877462.4 | 305307.0 | 34.8 | 21.8 |
| Total | 6530127.5 | 4268721.2 | 1397442.1 | 32.7 | 100.0 |

estimated by satellite data were higher than that estimated by Economic Affairs Sector, where the recorded values were 1397442.1 and 1308303.0 fed., respectively. Besides, the correlation coefficient results ($r=0.99$) indicated that there was a strong relationship between these tools. This means that satellite data are an excellent tool for estimating the cultivated rice area without the use of traditional tools used by the economic affairs sector in the survey of cultivated areas.

Also, the cultivated rice areas estimated by satellite data were higher than those reported by Economic Affairs Sector in four governorates (Sharkia, Behaira, Kafr Elsheik, and Gharbia) with a mean value of 38713.0, 26517.7, 16009.0 and 12887.9 fed., respectively. However, the rice-cultivated area in Dakahlia and Damietta that reported by Economic Affairs Sector was higher than that estimated by satellite data with mean values of 2407.9 and 2580.5 fed., respectively. These results are in agreement with those obtained

by Arafat et al. (2010) who found that estimated rice-cultivated area by satellite data (1550769.0 feds) was higher than that estimated area by Economic Affairs Sector (1061997.0 feds.). This over-cultivated area was assessed as 488771.0 feds. (46% of the total rice area).

This discrepancy in the obtained results could be attributed to many reasons. First of all, field-based methods applied by crop reporters are based on field size. However, they do not account for variability within each field. In some cases, the rice crop will have only emerged in one part of the field. A second important reason is the resolution of the satellite imagery (30 m). A solution to this problem would be the use of much higher resolution satellite imagery such as RapidEye (5 m) or Worldview-2 (1.84-m multispectral). However, this kind of imagery is not for free and was not available for this study. A third reason is that reported by Economic Affairs Sector relies on farmer surveys for the

Table 4 Comparison between rice-cultivated areas in the Nile Delta estimated by satellite data versus reported by economic affairs sector in 2016

| Governorates | Rice-cultivated area (Fed.) ^a | Rice-cultivated area (Fed.) ^b | Difference (Fed.) |
|---------------|--|--|-------------------|
| Behaira | 166293.0 | 192810.7 | +26517.7 |
| Kafr Elsheikh | 271699.0 | 287708.0 | +16009.0 |
| Dakahlia | 414449.0 | 412041.1 | -2407.9 |
| Damietta | 61365.0 | 58784.5 | -2580.5 |
| Gharbia | 127903.0 | 140790.9 | +12887.9 |
| Sharkia | 266594.0 | 305307.0 | +38713.0 |
| Total | 1308303.0 | 1397442.1 | 89139.1 |

T value = -2.246; p value = 0.075

Correlation value = 0.99; p value = 0.000

$R^2 = 0.9837$; $Y = 1.0017x + 14484$

^aEconomic affairs sector

^bSatellite data

area estimates instead of actual measurements, which introduces an additional source of error.

To validate the precision of the resultant rice maps, accuracy assessments of the resultant rice maps were conducted in three governorates through 600 field checkpoints throughout the rice-growing season; the results indicated that the resultant rice maps had high accuracies estimated by 97%. This accuracy could be attributed to the availability of satellite data at frequent intervals during the rice-growing season, which allows the possibility of traceability the rice crop during the different growth stages.

4 Conclusion

The satellite-based assessment is a good alternative and quick technique to monitor rice fields at a low cost. The remote sensing techniques could be sufficient methods to support the decision-makers with an accurate and timely efficient figure of the amount and the distribution of rice cultivation across the regional scale. The results showed that the total rice-cultivated area in the Nile Delta was accounted for 32.7% of the total cultivated area in all governorates. Dakahlia governorate had the most extensive area (29.5%) of the total rice-cultivated area, while the Damietta governorate recorded the lowest area (4.2%) of the total rice-cultivated area. The accuracy was high as 97% and 74% for LST and NDVI, respectively, which gives LST the advantage over NDVI.

References

- Abo-State MA, Ragab AME, EL-Gendy NS, Farahat LA, Madian HR (2014) Bioethanol production from rice straw enzymatically saccharified by fungal isolates, *Trichoderma Viride* F94 and *Aspergillus Terreus* F98. *Sci Res Publ* 3(2):19–29
- Arafat S, Afify A, Aboelghar M, Belal A (2010) Rice crop monitoring in Egyptian Nile delta using egyptsat-1 data. Joint US Egypt workshop for space technology and geo-information for sustainable development. NARSS, -Cairo, p 2010
- Blaschke T, Burnett C, Pekkarinen A (2004) Image segmentation methods for object-based analysis and classification. In: De Jong SM, Van D (eds) *Remote sensing image analysis: including the spatial domain*. Springer, Netherlands, pp 211–236
- Chavez PS (1996) Image-based atmospheric correction—revised and improved. *Photogram Eng Remote Sens* 62(9):1036–1052
- Chen G, Huang J, Hu J (2011) Mapping rice planting areas in southern China using the China environment satellite data. *Math Comput Model* 54(3–4):1037–1043
- Li P, Feng Z, Jiang L, Liu Y, Xiao X (2012) Changes in rice cropping systems in the Poyang lake region, China during 2004–2010. *J Geog Sci* 22(4):653–668
- Liang L, Gong P (2015) Evaluation of global land cover maps for cropland area estimation in the conterminous United States. *Int J Digit Earth* 8(2):102–117
- Liu L, Zhang X, Yu Y, Gao F, Yang Z (2018) Real-time monitoring of crop phenology in the Midwestern United States using VIIRS observations. *Remote Sens* 10(1540):1–18
- Mabrouk B, Abd-Elhamid HF, Badr M, Ludwig R (2013) Adaptation to the impact of sea level rise in the northeastern Nile delta, Egypt. *EGU Gen Assembl Conf* 15:4042
- Pan Y, Li L, Zhang J, Liang S, Zhu X, Sulla-Menashe D (2012) Winter wheat area estimation from MODISEVI time series data using the crop proportion phenology index. *Remote Sens Environ* 119:232–242. <https://doi.org/10.1016/j.rse.2011.10.011>
- Sakamoto T, Gitelson AA, Arkebauer TJ (2014) Near real-time prediction of US. Corn yields based on time-series MODIS data. *Remote Sens Environ* 147:219–231
- Saleh NHS (2016). Monitoring the agriculture land change and its impact on water consumption between Branches Damietta and Rosetta, Egypt using remote sensing and GIS techniques. PhD Thesis, Faculty of Women for Arts, Ain Shams University, Egypt
- Sinha S, Sharma LK, Nathawat MS (2015) Improved land-use/land-cover classification of semi-arid deciduous forest landscape using thermal remote sensing. *Egypt J Remote Sens Space Sci* 18:217–233
- Siyal AA, Dempewolf J, Becker-Reshef I (2015) Rice yield estimation using Landsat ETM+ data. *J Appl Remote Sens* 9(1):1–16
- Steel RGD, Torrie JH (1980) *Principles and Procedures of Statistics*, 2nd edn. McGraw Hill Book Co. Inc, New York
- Valor E, Caselles V (1996) Mapping land surface emissivity from NDVI: application to European, African, and south American areas. *Remote Sens Environ* 57(3):167–184
- Zhang G, Xiao X, Dong J, Kou W, Jin C, Qin Y, Biradar C (2015) Mapping paddy rice planting areas through time series analysis of MODIS land surface temperature and vegetation index data. *ISPRS J Photogramm Remote Sens* 106:157–171
- Zhang X, Zhang M, Zheng Y, Wu B (2016) Crop mapping using PROBA-V time series data at the Yucheng and Hongxing farm in China. *Remote Sens* 8(11):915